

# Prevention Of Outages In Power Systems With Distributed Generation Plants

Yuri Bulatov<sup>1,\*</sup>, Andrey Kryukov<sup>2</sup>

<sup>1</sup> Bratsk State University, Bratsk, Russia.

<sup>2</sup> Irkutsk State Transport University, Irkutsk National Research Technical University, Irkutsk, Russia

**Abstract**— The paper is concerned with the study aimed at the development of methods for emergency control in power systems with distributed generation plants. The control actions enabling the state parameters to meet stability constraints were generated by changing the vector of controlled parameters along a preset path corresponding to the shortest distance from a point of the initial state to a limiting hypersurface. In this case, limit loads equations of the power system were used. The quality of dynamic processes during control actions was ensured by harmonized tuning of the automatic voltage regulator (AVR) and automatic speed regulator (ASR) of distributed synchronous generators. Computer-aided modeling was used to demonstrate that the post-emergency operating conditions meeting stability constraints can be calculated using limit load equations while using the starting algorithm that enables the values of operating parameters to reach the nearest boundary of the feasibility (stability) region. Modeling of the power system in MATLAB environment demonstrates that the fuzzy algorithms used to control AVR and ASR settings considerably enhance the quality of transient processes of voltage, frequency, and power when the power of distributed generators in post-emergency conditions is reduced.

**Index Terms** — power supply systems, distributed generation plants, emergency control, harmonized setting, automatic voltage regulator, automatic speed regulator.

## I. INTRODUCTION

The use of intelligent electric power systems (EPS) with active-adaptive networks implies the active use of distributed generation (DG) plants located in the immediate vicinity of power consumers. The following facilities can be referred to as the DG plants:

- unconventional renewable energy sources: solar panels, wind generating plants, fuel cells, and others;
- small- and medium-capacity cogeneration plants (small thermal power plants based on gas turbine and combined cycle gas turbine technologies), as well as mini- and micro-hydro power plants.

Active use of DG technologies in EPS requires new algorithms and systems for control in normal, emergency and post-emergency conditions [1 – 4] to provide the required stability and quality of the dynamic transition.

A main function of emergency control (EC) systems is to ensure static non-oscillatory stability of post-emergency conditions (PEC) of EPS. In this case, the control actions are generated to provide the PEC parameters meeting the feasibility (stability) constraints along a certain trajectory  $DY$  in the space of controlled parameters  $Y$  [5 – 7]. Normally, the trajectory  $DY$  is assumed to be linear and can be determined either by setting based on the preliminary calculations; or based on the condition of the shortest distance to a limiting hypersurface or according to the minimum damage caused by disconnecting power sources and consumers.

The use of DG plants makes the calculation of operating conditions meeting stability constraints relevant to the distribution networks and power supply systems. This is of special importance in electric power systems equipped with DG plants based on unconventional renewable energy sources. Such plants, as mini hydropower plants and offshore windmill farms, can be located at a distance from the load centers, which ‘narrows’ the static non-oscillatory stability areas.

When set optimally, the automatic regulators of distributed generators can ensure the necessary oscillatory

\* Corresponding author.

E-mail: [bulatovyura@yandex.ru](mailto:bulatovyura@yandex.ru)

<http://dx.doi.org/10.25729/esr.2019.01.0008>

Received March 28, 2019. Revised April 22, 2019.

Accepted May 18, 2019. Available online June 25, 2019.

This is an open access article under a Creative Commons Attribution-NonCommercial 4.0 International License.

© 2019 ESI SB RAS and authors. All rights reserved.

stability margin and quality dynamic transition in emergency and post-emergency conditions. Optimal adaptive control of DG plants in different conditions can be achieved by using advanced intelligent technologies [8 – 18].

The paper describes a DG emergency control system which, in contrast to the approaches described in [2, 5, 7], is based on determination of the post-emergency conditions that meet the stability constraints with the limit load equations and a fuzzy control system for tuning the controllers of the DG plants in emergency and post-emergency conditions that provide a qualitative dynamic transition. This makes it possible to maintain the steady-state and dynamic stability of power supply systems with distributed generators.

## II. PROBLEM STATEMENT

The emergency control is illustrated in Fig. 1, where the stability region is cut by the coordinate plane of generator active powers  $P_i, P_j$ . In this Figure, it is assumed that the stability and transmitted power limits coincide [7]. Curve 1 corresponds to the boundary of the stability region for the complete network diagram, Curve 2 corresponds to a similar boundary when one of the main transmission lines is disconnected, and curve 3 corresponds to the condition  $\Im = \text{const}$ , where  $\Im$  is the required value of the stability margin of the post-emergency conditions.

The aim of the emergency control application is to reach one of the points:  $\mathbf{Y}_z^{(1)}, \mathbf{Y}_z^{(2)}, \mathbf{Y}_z^{(3)}$

$$\mathbf{Y}_z^{(1)} = \mathbf{Y}_0 + D\mathbf{Y}^{(1)} = \mathbf{Y}_0 + t_1 \Delta \mathbf{Y}^{(1)},$$

$$\mathbf{Y}_z^{(2)} = \mathbf{Y}_0 + D\mathbf{Y}^{(2)} = \mathbf{Y}_0 + t_2 \Delta \mathbf{Y}^{(2)},$$

$$\mathbf{Y}_z^{(3)} = \mathbf{Y}_0 + D\mathbf{Y}^{(3)} = \mathbf{Y}_0 + t_3 \Delta \mathbf{Y}^{(3)}, \text{ where } D\mathbf{Y}^{(k)}, k = 1..3$$

– the trajectories of the condition change in space  $\mathbf{Y}$ ;  $\Delta \mathbf{Y}^{(k)}, k = 1..3$  – directions of the condition change;

$t_k, k = 1..3$  – scalar parameters that determine the amount of generator power reduction in the relevant direction; index  $k = 1$  corresponds to the direction set a priori, index  $k = 2$  corresponds to power reduction in the direction of the normal to the limiting hypersurface, while  $k = 3$  – corresponds to power reduction ensuring minimal possible damage caused by disconnection of power sources and consumers [5 – 7].

Power should be reduced in the chosen direction  $\Delta \mathbf{Y}^{(k)}$  with an acceptable quality of the dynamic processes, which can be achieved through the use of automatic voltage regulator (AVR) and automatic speed regulator (ASR) in the synchronous generators of DG plants. The relatively small power of DG plants and the small constant value of DG plants rotor inertia require that the mutual influence of AVR and ASR be taken into account when tuning them. It should also be noted, that the optimal control requires the adjustment of AVR and ASR settings when the operating conditions change greatly in both DG and power supply systems.

Below are the results of the studies aimed at the

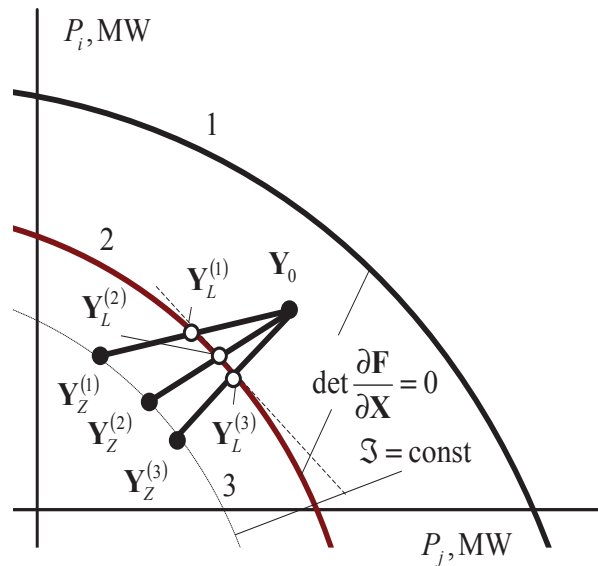


Fig. 1. Determination of post-emergency conditions meeting stability constraints:  $\frac{\partial F}{\partial X}$  – matrix of Jacobi for steady-state equations (SSE);  $\Im$  – stability margin

development of methods for determining the post-emergency operating conditions that meet the stability constraints and for ensuring a quality dynamic transition when generator power is reduced.

## III. METHODS FOR DETERMINING POST-EMERGENCY OPERATING CONDITIONS MEETING STABILITY CONSTRAINTS

The emergency control system of distributed generation plants is intended to ensure stable operation of generators in electric power system in post-emergency conditions, in which case the parameters of the conditions meeting the stability constraints can be determined by different methods, for instance, a method based on limit loads equations (LLE) [7, 19, 20] whose derivation is described below.

The equilibrium position of the autonomous system of differential equations  $\frac{dx_i}{dt} = w_i(x_1, x_2, \dots, x_n) \quad i = \overline{1..n}$ , (1) is asymptotically stable according to Lyapunov, if the linearized system (initial approximation system) is stable too:

$$\frac{dx_i}{dt} = \sum_{k=1}^n \left( \frac{\partial w_i}{\partial x_k} \right)_{x_k=x_{k0}} \Delta x_k, \quad i = \overline{1..n} \quad (2)$$

where  $\Delta x_k = x_k - x_{k0}$ ;  $x_{k0}$  – equilibrium point coordinates

satisfying the equations

$$w_i(x_{10}, x_{20}, \dots, x_{n0}) = 0; \quad i = \overline{1..n}.$$

The linearization procedure is performed based on the expansion of functions  $w_i(x_1, x_2, \dots, x_n), i = \overline{1..n}$  in Taylor's series

$$w_i(x_1, x_2, \dots, x_n) = w_i(x_{10}, x_{20}, \dots, x_{n0}) + \sum_{k=1}^n \left( \frac{\partial w_i}{\partial x_k} \right)_{x=x_0} \Delta x_k + \\ + \frac{1}{2!} \sum_{k=1}^n \sum_{j=1}^n \left( \frac{\partial^2 w_i}{\partial x_k \partial x_j} \right) \Delta x_k \Delta x_j + \dots$$

and rejection of nonlinear terms.

Solutions to equations (2) are stable if real parts of all roots of the standard equation are negative

$$D(p) = \det \left( \frac{\partial \mathbf{W}}{\partial \mathbf{X}} - p \mathbf{E} \right) = 0 \quad (3)$$

where  $\frac{\partial \mathbf{W}}{\partial \mathbf{X}}$  the Jacobian matrix of  $\mathbf{W}(\mathbf{X})$  calculated at the equilibrium point

$$\frac{\partial \mathbf{W}}{\partial \mathbf{X}} = \begin{bmatrix} \frac{\partial w_1}{\partial x_1} & \dots & \frac{\partial w_1}{\partial x_n} \\ \frac{\partial w_2}{\partial x_1} & \dots & \frac{\partial w_2}{\partial x_n} \\ \vdots & \ddots & \vdots \\ \frac{\partial w_n}{\partial x_1} & \dots & \frac{\partial w_n}{\partial x_n} \end{bmatrix}$$

$\mathbf{E} = \text{diag}1$  – an identity matrix of order n. Equilibrium will be unstable if equation (2) has at least one root with a positive real part. If there are no such roots but there are just imaginary ones, then the system of initial approximation cannot be used to judge about stability. In this case, an additional study is required.

With regard to steady states of EPS, the stability according to Lyapunov, which is called steady-state stability, is subdivided according to the nature of disturbance into non-oscillatory (aperiodic) and oscillatory stability. The first type of instability is associated with the appearance of positive real roots, while the second type – with the emergence of complex roots with a positive real part. Practical methods for determining the non-oscillatory and oscillatory stability differ from one another. Below, we analyze only the methods and criteria that are used to determine the non-oscillatory instability.

In order for the standard equation (3) that can be represented in the following expanded form with regard to p symbol

$$D(p) = p^n + a_{n-1}p^{n-1} + \dots + a_0 = 0 \quad (4)$$

not to have real positive roots  $p_k$ , it is necessary and sufficient that all coefficients (4) be higher than zero. However, if stability limit is determined in the process of load increase with respect to initial steady state, there is no need to follow the signs of all coefficients, because the constant term  $a_0$  of the characteristic polynomial will be the first to change the sign for negative.

Indeed, it follows from (3) and (4) that

$$a_0 = (-1)^n \det \frac{\partial \mathbf{W}}{\partial \mathbf{X}} \quad (5)$$

and  $a_0 = 0$  when  $p_k = 0$ .

Therefore, with changes in the real root value from

negative to positive, the change in the sign of  $a_0$  is inevitable. The sign control of the constant term of a characteristic polynomial is the basis for the main methods used to determine stability-limited conditions.

The electrical power system steady states are defined by non-linear equations of the type

$$\mathbf{F}(\mathbf{X}, \mathbf{Y}) = \mathbf{0} \quad (6)$$

where  $\mathbf{F} = [f_1 f_2 \dots f_n]^T$  – n-dimensional vector function, satisfying the balance equations of power or currents at network nodes;  $\mathbf{Y} = [y_1 y_2 \dots y_m]^T$  – the set vector of regulated parameters (independent variables);  $\mathbf{X} = [x_1 x_2 \dots x_n]^T$  – required vector of non-regulated parameters (dependent variables).

Active and reactive powers of generators and loads, as well as voltage magnitudes observed at some network nodes, are usually used as controlled parameters. Dependent variables are real and imaginary components or magnitudes and phases of nodal voltages. EPS frequency value can also be part of  $\mathbf{X}$  dependable variables vector.

The EPS loads corresponding to the points of parameter space  $\mathbf{Z} = \mathbf{X} \cup \mathbf{Y}$ , at which equations (1) and condition

$$a_0 = (-1)^n \det \frac{\partial \mathbf{W}}{\partial \mathbf{X}} = 0 \quad (7)$$

are satisfied can be considered to be steady-state non-oscillatory stability-limited conditions, where  $\mathbf{W}$  – n-dimensional vector function, corresponding to right-hand sides of differential equations

$$\frac{d\mathbf{X}}{dt} = \mathbf{W}(\mathbf{X}, \mathbf{Y}) \quad (8)$$

that describe transient processes in EPS for small-scale disturbances;  $a_0$  – the constant term of the characteristic polynomial

$$\det \left( p \mathbf{E} - \frac{\partial \mathbf{W}}{\partial \mathbf{X}} \right) = 0$$

The expression for  $a_0$  can be obtained without generation of differential equations, but immediately from steady-state equations (SSE).

$$\mathbf{W}(\mathbf{X}, \mathbf{Y}) = \mathbf{0} \quad (9)$$

written considering characteristics of the electrical system components for small-scale disturbances.

Points satisfying condition (5) form discriminant hypersurface  $L_W$  in space  $\mathbf{Y}$  (Fig. 2).

The conditions can be considered to be limited by the existence (transmitted power) when they correspond to the parameter space points  $\mathbf{Z} = \mathbf{X} \cup \mathbf{Y}$ , at which steady-state equations (6) and the condition

$$\det \frac{\partial \mathbf{F}}{\partial \mathbf{X}} = 0 \quad (10)$$

are satisfied, where  $\frac{\partial \mathbf{F}}{\partial \mathbf{X}}$  – the Jacobian matrix for the steady-state equation (6).

Points satisfying condition (10) form the discriminant hypersurface  $L_F$  in space  $\mathbf{Y}$  (Fig. 2).

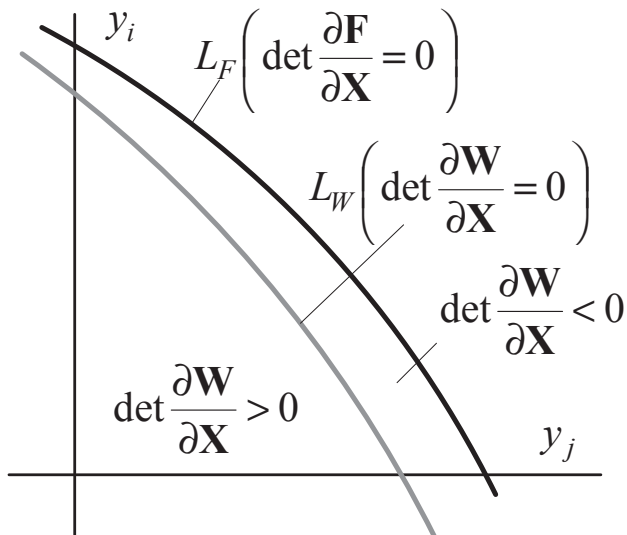


Fig. 2. Regions of stability and existence of conditions in space of parameters  $\mathbf{Y}$ .

In a general case, matrices of Jacobi  $\frac{\partial \mathbf{F}}{\partial \mathbf{X}}$  that are used to determine steady-state parameters, and matrices  $\frac{\partial \mathbf{W}}{\partial \mathbf{X}}$  that are used for stability analysis can fail to coincide for the following reasons:

1. Steady-state equations (6) can be written for various assumptions and in various forms, which, in the general case, do not coincide with those made to write differential equations (8).
2. Based on the assumption that astatic control of voltage  $U_G$  at generator buses is performed by changing the settings of automatic voltage regulators, the magnitude of  $U_G$  for calculations of operating conditions is normally assumed to be given. If such a control is performed by dispatcher discretely, then the supposition on voltage stability at generator buses, which is quite admissible for the calculation of operating conditions, will be unsatisfactory for the determination of stability. In this case, it would be more correct to assume generator electromotive force to be constant with some reactance determined depending on type and values of AVR amplification factors or to fully take into account the mathematical formulation of the excitation control law. In the case of sufficiently high AVR amplification factors, both methods of generator modeling lead to the same results.
3. When the substations that power the consumer have transformers with on-load voltage regulation, the load power can be considered constant in the calculations of operating conditions. Contrastingly, in an analysis of stability, the load power should be assumed to be changeable as per static characteristics, because the said control is of discrete nature and does not work in the case of small-scale disturbances.

An analysis carried out in [7] shows that despite the development of a number of effective algorithms, the problem of express calculation of operating conditions that are limiting in terms of their static stability and transmitted power remains relevant. The technique for determining the limiting conditions, which does not require multi-step computational procedures, which is applicable whether or not the transmitted power and stability limits coincide, and which allows avoiding the difficulties in solving ill-conditioned systems, can be implemented on the basis of the LLE and their generalizations [7, 19, 20].

This technique is based on the replacement of condition (5) with an equivalent ratio which can be represented in two ways:

$$\mathbf{VS} = \frac{\partial \mathbf{W}}{\partial \mathbf{X}} \mathbf{S} = \mathbf{0} \quad (11)$$

$$\mathbf{VR} = \left( \frac{\partial \mathbf{W}}{\partial \mathbf{X}} \right)^T \mathbf{R} = \mathbf{0} \quad (12)$$

where  $\mathbf{VS}$ ,  $\mathbf{VR}$  –  $n$ -dimensional vector functions;

$$\mathbf{S} = [s_1 \ s_2 \ \dots \ s_n]^T; \quad \mathbf{R} = [r_1 \ r_2 \ \dots \ r_n]^T \quad -$$

respectively, eigenvectors of matrices  $\frac{\partial \mathbf{W}}{\partial \mathbf{X}}, \left( \frac{\partial \mathbf{W}}{\partial \mathbf{X}} \right)^T$  that satisfy zero eigenvalues.

Since (11) and (12) define the eigenvectors to the accuracy of constant factor, one of their components can be assumed to be arbitrary, different from zero. For example,  $r_n = s_n = 1$ . Another way for the extension of definition for equations (11) and (12) is to set a length, for example, unit length for vectors  $\mathbf{R}$  and  $\mathbf{S}$ , that is, to supplement these systems with the equations:  $U(\mathbf{S}) = \mathbf{S}^T \mathbf{S} - 1 = 0$  or  $U(\mathbf{R}) = \mathbf{R}^T \mathbf{R} - 1 = 0$

The Jacobian matrices elements are the functions of dependable parameters  $\mathbf{X}$ . Consequently, unlike (7), conditions (11) and (12) allow an analytical description of hypersurface  $LW$  of limiting conditions.

Determination of static stability-limited conditions is reduced to simultaneously solving the sets of equations which can be represented in two ways

$$\left. \begin{aligned} \mathbf{F}[\mathbf{X}, \mathbf{Y}(t)] &= \mathbf{0}; \\ \mathbf{VS}[\mathbf{X}, \mathbf{S}, \mathbf{Y}(t)] &= \frac{\partial \mathbf{W}}{\partial \mathbf{X}} \mathbf{S} = \mathbf{0}; \\ U(\mathbf{S}) &= \mathbf{S}^T \mathbf{S} - 1 = 0. \end{aligned} \right\} \quad (13)$$

or

$$\left. \begin{aligned} \mathbf{F}[\mathbf{X}, \mathbf{Y}(t)] &= \mathbf{0}, \\ \mathbf{VR}[\mathbf{X}, \mathbf{R}, \mathbf{Y}(t)] &= \left( \frac{\partial \mathbf{W}}{\partial \mathbf{X}} \right)^T \mathbf{R} = \mathbf{0}, \\ U(\mathbf{R}) &= \mathbf{R}^T \mathbf{R} - 1 = 0, \end{aligned} \right\} \quad (14)$$

where  $\mathbf{F}$  –  $\ell$ -dimensional vector function satisfying steady-state equations;  $\mathbf{X}$  –  $\ell$ -dimensional vector of uncontrolled

parameters;  $\mathbf{Y}$  –  $m$ -dimensional vector of controlled parameters;  $\mathbf{Y}(t) = \mathbf{Y}_0 + t\Delta\mathbf{Y}$ ;  $\mathbf{Y}_0$  – the value of vector of controlled parameters in the initial (pre-emergence) conditions;  $\mathbf{R}$  – eigenvector of matrix  $\left(\frac{\partial\mathbf{W}}{\partial\mathbf{X}}\right)^T$  satisfying zero eigenvalue. In the case where the limits of stability and transmitted power coincide, matrix  $\frac{\partial\mathbf{F}}{\partial\mathbf{X}}$  is used instead of matrix  $\frac{\partial\mathbf{W}}{\partial\mathbf{X}}$ .

Systems (13) and (14) are equivalent, however, in equations (14), eigenvector  $\mathbf{R}$ , which coincides with the direction of normal to hypersurface  $L_W$ , is used. This makes it possible to generalize the limit load equations for the case of their search in the most dangerous (critical) direction of load increase that corresponds to the shortest distance in the metrics of normalized independent variables from the point of the considered conditions to the limit hypersurface, and thus to obtain an objective estimate for the static non-oscillatory stability margin. For this reason, below, the equations of limit loads are considered in the form of (14). Multiple calculation experiments [7] show that equations (14) can be used to calculate the operating conditions of an electric power system to reach the boundary of the stability region: the point  $\mathbf{Y}_L^{(1)}$  (Fig. 1). To achieve the required stability margin, power should be additionally reduced in the direction of  $\Delta\mathbf{Y}^{(1)}$  (point  $\mathbf{Y}_Z^{(1)}$ ) or in the direction of vector  $\mathbf{R}$ , Fig. 3.

It is worth noting that the two-stage procedure refers only to the algorithm of determining the point  $\mathbf{Y}_Z^{(R)}$ , whereas dynamic transition is performed directly from point  $\mathbf{Y}_0$  to point  $\mathbf{Y}_Z^{(R)}$ .

The post-emergency conditions meeting the stability constraints can be calculated with respect to the shortest path by modifying the limit load equations, which is intended to search for the limit load in the critical direction

of load increase [7, 20]. Provided the limits of stability and transmitted power coincide, this problem can be formulated as follows:

Find

$$\mathfrak{I}_{min} = \min(D\mathbf{Y}^T \mathbf{M}^2 D\mathbf{Y})^{\frac{1}{2}} \quad (15)$$

subject to

$$\mathbf{F}(\mathbf{X}, \mathbf{Y}_0 + D\mathbf{Y}) = \mathbf{0} \quad (16)$$

where  $\mathbf{Y}_0$  – vector of controlled parameters in the initial (pre-emergence) conditions;  $D\mathbf{Y} = [dy_1 \ dy_2 \ \dots \ dy_n]^T$  – incremental vector of variables  $\mathbf{Y}_0$  which ensure that the operating conditions attain the hypersurface  $L_F$ ;  $\mathbf{M} = \text{diag}\mu_i, \mu_i$  – scaling factors.

To solve the formulated problem (assuming that the limits of stability and the transmitted power coincide), the Lagrange function is written as follows

$$L(\mathbf{X}, \mathbf{Y}_0 + D\mathbf{Y}, \boldsymbol{\Lambda}) = (D\mathbf{Y}^T \mathbf{M}^2 D\mathbf{Y})^{\frac{1}{2}} + \mathbf{F}^T(\mathbf{X}, \mathbf{Y}_0 + D\mathbf{Y})\boldsymbol{\Lambda}$$

where  $\boldsymbol{\Lambda}$  – the undetermined multiplier vector.

The  $L$  minimum corresponds to the conditions

$$\begin{aligned} \frac{\partial L}{\partial D\mathbf{Y}} &= \mathbf{M}^2 D\mathbf{Y} (D\mathbf{Y}^T \mathbf{M}^2 D\mathbf{Y})^{-\frac{1}{2}} + \left( \frac{\partial \mathbf{F}}{\partial D\mathbf{Y}} \right)^T \boldsymbol{\Lambda} = \mathbf{0} \\ \frac{\partial L}{\partial \mathbf{X}} &= \left( \frac{\partial \mathbf{F}}{\partial \mathbf{X}} \right)^T \boldsymbol{\Lambda} = \mathbf{0}; \\ \frac{\partial L}{\partial \boldsymbol{\Lambda}} &= \mathbf{F}(\mathbf{X}, \mathbf{Y}_0 + D\mathbf{Y}) = \mathbf{0}. \end{aligned} \quad (17)$$

The first equation of the system corresponds to the shortest distance  $\mathfrak{I}_{min}$  from the point  $\mathbf{Y}_0$  to hypersurface  $L_F$  in metrics set by  $\mathbf{M}$  matrix. The second equation of the system ensures that the operating conditions correspond to the hypersurface  $\mathfrak{I}_{min}$  for non-zero  $\boldsymbol{\Lambda}$ . The third equation of the system corresponds to the balanced operating conditions.

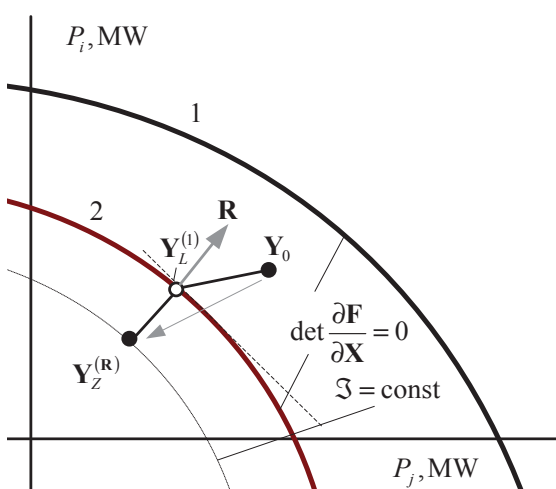


Fig. 3. Additional power reduction in the direction of vector  $\mathbf{R}$ .

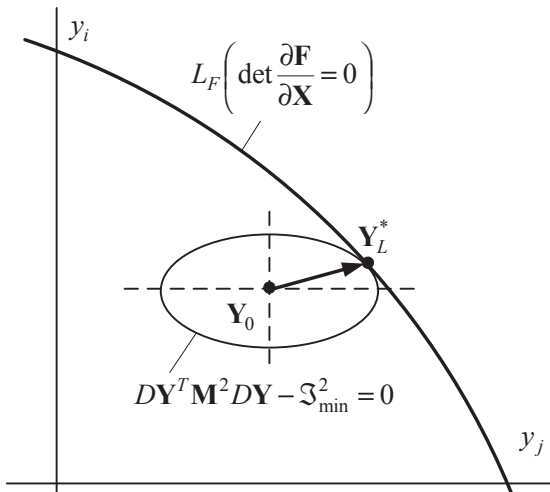


Fig. 4. Geometrical interpretation of search for a critical direction of load increase.

Geometrically, the solution to system (17) is the contact point of hypersurface  $L_F$  and ellipsoid with the center at point  $\mathbf{Y}_0$  (Fig. 4), defined by the equation:

Geometrically, the solution to system (17) is the contact point of hypersurface and ellipsoid with the center at point (Fig. 4), defined by the equation:  $D\mathbf{Y}^T \mathbf{M}^2 D\mathbf{Y} - \mathfrak{I}_{\min}^2 = 0$

Equations (17) can be represented as follows:

$$\frac{\partial L}{\partial D\mathbf{Y}} = \mathbf{M}^2 D\mathbf{Y} + \left( \frac{\partial \mathbf{F}}{\partial D\mathbf{Y}} \right)^T \mathbf{A} (D\mathbf{Y}^T \mathbf{M}^2 D\mathbf{Y})^{\frac{1}{2}} = \mathbf{0}$$

$$\frac{\partial L}{\partial \mathbf{X}} = \left( \frac{\partial \mathbf{F}}{\partial \mathbf{X}} \right)^T \mathbf{A} = \mathbf{0}$$

$$\frac{\partial L}{\partial D\mathbf{Y}} = \mathbf{F}(\mathbf{X}, \mathbf{Y}_0 + D\mathbf{Y}) = \mathbf{0}$$

Vector  $\mathbf{A}$  is determined with the accuracy of the multiplier, consequently the variables can be replaced

$$\mathbf{R} = \mathfrak{I}_{\min} \mathbf{A} = \mathbf{A} (D\mathbf{Y}^T \mathbf{M}^2 D\mathbf{Y})^{\frac{1}{2}}$$

then

$$\frac{\partial L}{\partial D\mathbf{Y}} = \mathbf{M}^2 D\mathbf{Y} + \left( \frac{\partial \mathbf{F}}{\partial D\mathbf{Y}} \right)^T \mathbf{R} = \mathbf{0}$$

$$\frac{\partial L}{\partial \mathbf{X}} = \left( \frac{\partial \mathbf{F}}{\partial \mathbf{X}} \right)^T \mathbf{R} = \mathbf{0}$$

$$\frac{\partial L}{\partial D\mathbf{Y}} = \mathbf{F}(\mathbf{X}, \mathbf{Y}_0 + D\mathbf{Y}) = \mathbf{0}$$

After determining from the first equation

$$D\mathbf{Y} = -\mathbf{M}^{-2} \left( \frac{\partial \mathbf{F}}{\partial D\mathbf{Y}} \right)^T \mathbf{R}$$

and after substituting it in the third equation, we can obtain a system representing the modification of the limit load equation which makes it possible to calculate the post-emergency conditions meeting the stability constraints based on the shortest path:

$$\left. \begin{aligned} & \mathbf{F} \left( \mathbf{X}, \mathbf{Y}_0 - \mathbf{M}^{-2} \left( \frac{\partial \mathbf{F}}{\partial D\mathbf{Y}} \right)^T \mathbf{R} \right) = \mathbf{0}; \\ & \mathbf{V}\mathbf{R}(\mathbf{X}, \mathbf{R}) = \left( \frac{\partial \mathbf{F}}{\partial \mathbf{X}} \right)^T \mathbf{R} = \mathbf{0}. \end{aligned} \right\} \quad (18)$$

If vector components  $D\mathbf{Y}$  belong to the first group of equations (18) linearly, then  $\left( \frac{\partial \mathbf{F}}{\partial D\mathbf{Y}} \right)^T = \mathbf{E}$

This takes place when steady-state equations written in a Cartesian coordinate system can be represented as:

$$f_{2i-1}(\mathbf{X}, \mathbf{Y}) = P_{i0} + dP_i - P_{ci}(U'_1 U''_1 \dots U'_p U''_p) = 0;$$

$$f_{2i}(\mathbf{X}, \mathbf{Y}) = Q_{i0} + dQ_i - Q_{ci}(U'_1 U''_1 \dots U'_p U''_p) = 0,$$

where  $P_{i0}, Q_{i0}$  – power injections in the initial conditions;

$U'_i, U''_i$  – real and imaginary components of nodal voltage;

$dP_i, dQ_i$  – vector components  $D\mathbf{Y}$ ;  $p$  – the number of network nodes except for the slack node. With an implicit

$\mathbf{X}$  dependence of  $\mathbf{Y}$ , the  $\left( \frac{\partial \mathbf{F}}{\partial D\mathbf{Y}} \right)^T$  matrix is block-diagonal and its elements are determined by the formulas given in [7].

When Newton's method is used to solve equations (18), the following system of linear equations is solved at each iteration:

$$\left[ \begin{array}{cc} \frac{\partial \mathbf{F}}{\partial \mathbf{X}} & \frac{\partial \mathbf{F}}{\partial \mathbf{R}} \\ \frac{\partial \mathbf{V}\mathbf{R}}{\partial \mathbf{X}} & \frac{\partial \mathbf{V}\mathbf{R}}{\partial \mathbf{R}} \end{array} \right] \begin{bmatrix} \Delta \mathbf{X} \\ \Delta \mathbf{R} \end{bmatrix} = - \begin{bmatrix} \mathbf{F} \\ \mathbf{V}\mathbf{R} \end{bmatrix}$$

$$\text{where } \frac{\partial \mathbf{F}}{\partial \mathbf{R}} = \mathbf{M}^{-2} \left( \frac{\partial \mathbf{F}}{\partial D\mathbf{Y}} \right)^T; \quad \frac{\partial \mathbf{V}\mathbf{R}}{\partial \mathbf{R}} = \left( \frac{\partial \mathbf{F}}{\partial \mathbf{X}} \right)^T$$

Modeling shows that based on equations (18), the electric power system operating conditions can be calculated to meet the boundary stability constraint using the shortest path: the point  $\mathbf{Y}_L^{(2)}$  (Fig. 1). To achieve the required margin, power should be additionally reduced.

In some cases of using equations 14 or 18, however, the ‘remote boundary’ of the stability region can be achieved [21], i.e. the point  $\mathbf{Y}_L^{(db)}$  in Fig. 5. In this case, the obtained solution differs in the inversion of power injection signs, and cannot be used in practice.

An effective method to cope with the ‘remote boundary’ problem can be implemented based on starting algorithms, which employ special methods of solving the steady-state equations [19, 22].

The starting algorithm, in particular, can be based on V.A. Matveev method whose iterative formula has the form

$$\mathbf{X}^{(k+1)} = \mathbf{X}^{(k)} - \lambda^{(k)} \left[ \frac{\partial \mathbf{F}}{\partial \mathbf{X}}(\mathbf{X}^{(k)}) \right]^{-1} \mathbf{F}(\mathbf{X}^{(k)}) \quad (19)$$

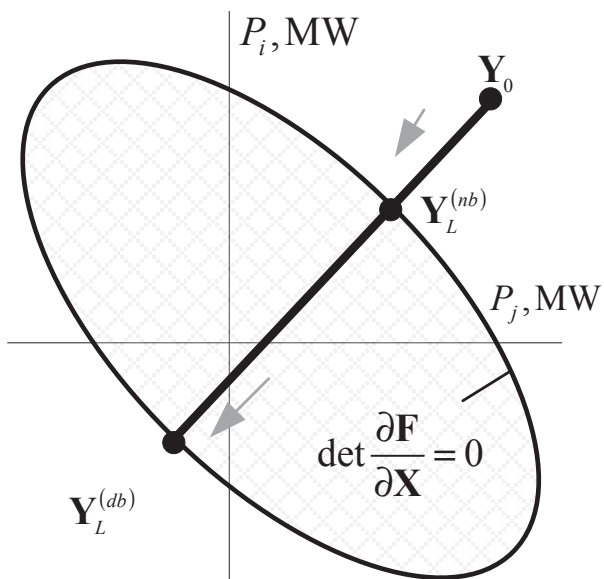


Fig. 5. To the problem of the ‘remote boundary’ of the stability region.

where  $\lambda^{(k)}$  – an adjusting factor, determined by the expression

$$\lambda^k = \begin{cases} \frac{1}{B_k}, & \text{if } B_k > 1 \\ 1, & \text{if } B_k \leq 1 \end{cases}$$

$$B_k = \frac{1}{2\max|\mathbf{F}(\mathbf{X}^{(k)})|} \max \left| \sum_{(i)} \sum_{(j)} \frac{\partial^2 f_i(\mathbf{X}^{(k)})}{\partial x_i \partial x_j} \Delta x_j^{(k)} \Delta x_i^{(k)} \right|$$

The second multiplier for  $B_k$  is the maximum absolute value of the vector component obtained by multiplying the matrix of the second derivatives of vector-function  $\mathbf{F}(\mathbf{X})$  by the elements of correction vector  $\Delta\mathbf{X}$  that are determined at the  $k$ -th iteration. The iterative procedure (19) ensures the convergence of the computational process for any existing conditions, while when nonexistent conditions are calculated, the calculation process "hangs" at the point of the limiting hypersurface, where the Jacobian of the system of steady-state equations equals zero.

Another starting algorithm can be implemented based on the computational methods [19], which additionally take into account the higher-order terms of the Taylor series expansion of the vector-function  $\mathbf{X}=\Phi(\mathbf{Y})$  inverse to  $\mathbf{F}(\mathbf{X})$ .

Based on the expansion,  $\mathbf{X}$  is represented as

$$\mathbf{X} = \mathbf{X}_0 + \Delta\mathbf{X}_1(\Delta\mathbf{F}) + \Delta\mathbf{X}_2(\Delta\mathbf{F}^2) + \dots + \Delta\mathbf{X}_k(\Delta\mathbf{F}^k) + \dots$$

where  $\Delta\mathbf{X}_k(\Delta\mathbf{F}^r)$  – correction vectors, depending on products of vector components

$$\Delta\mathbf{F} = \mathbf{F}(\mathbf{X}) - \mathbf{F}(\mathbf{X}_0) \quad (20)$$

with the sum of powers equal to  $r$ . Besides, at the point of solution, it is necessary to assume  $\Delta\mathbf{F} = -\mathbf{F}(\mathbf{X}_0)$ .

Corrections  $\Delta\mathbf{X}_p$  are calculated using the recurrent expressions:

$$\Delta\mathbf{X}_1^{(k)} = - \left[ \frac{\partial \mathbf{F}}{\partial \mathbf{X}}(\mathbf{X}^{(k)}) \right]^{-1} \mathbf{F}(\mathbf{X}^{(k)})$$

$$\Delta\mathbf{X}_2^{(k)} = \left[ \frac{\partial \mathbf{F}}{\partial \mathbf{X}}(\mathbf{X}^{(k)}) \right]^{-1} \mathbf{B}_2^{(k)}$$

$$\Delta\mathbf{X}_3^{(k)} = \left[ \frac{d\mathbf{F}}{d\mathbf{X}}(\mathbf{X}^{(k)}) \right]^{-1} \mathbf{B}_3^{(k)}$$

where  $k$  – iteration number;  $\Delta\mathbf{X}_r^{(k)}$  – vector of  $r$ -th corrections;  $r = 1 \dots 3$ .

Components of vectors

$$\mathbf{B}_r^{(k)} = [b_{r1}^{(k)} \ b_{r2}^{(k)} \ \dots \ b_{ri}^{(k)} \ \dots \ b_m^{(k)}]^T,$$

which are parts of expressions for the second and third corrections, are calculated using the formula

$$b_{2i}^{(k)} = [\Delta\mathbf{X}_1^{(k)}]^T \boldsymbol{\Gamma}_i^{(k)} \Delta\mathbf{X}_1^{(k)}; \ b_{3i}^{(k)} = [\Delta\mathbf{X}_1^{(k)}]^T \boldsymbol{\Gamma}_i^{(k)} \Delta\mathbf{X}_2^{(k)},$$

where  $\boldsymbol{\Gamma}_i^{(k)}$  – Hessian matrix of the function  $f_i(\mathbf{X})$ , calculated at the point  $\mathbf{X}^{(k)}$ .

The first correction coincides with the one determined by Newton's method and corresponds to the linear approximation of  $\mathbf{X}$  from  $\Delta\mathbf{F}$ . The second and subsequent corrections correspond to the approximation of  $\mathbf{X}$  with polynomials of a higher degree, hence the acceleration of the iteration process when the number of considered corrections increases.

In the presented form, the method under consideration, due to the poor convergence of the series  $\mathbf{X}^{(k)} = \mathbf{X}_0 + \sum_r \Delta\mathbf{X}_r$

with the initial approximations chosen 'far' from the solution, gives a less reliable calculation of 'heavy' loads than Newton's method. An increase in the reliability of the method is associated with the improvement in the convergence of the indicated series, and to this end, the correction factors are introduced as follows. Instead of search for the point of the solution  $\mathbf{X}_p$ , where  $\mathbf{F}(\mathbf{X}_p) = \mathbf{0}$ , we determine an intermediate point  $\mathbf{X}^*$  with the value of the function of residuals

$$\mathbf{F}(\mathbf{X}^*) = (1-\alpha)\mathbf{F}(\mathbf{X}_0), \alpha < 1$$

Substitution

$$\Delta\mathbf{F} = \mathbf{F}(\mathbf{X}^*) - \mathbf{F}(\mathbf{X}_0) = -\alpha\mathbf{F}(\mathbf{X}_0)$$

in (20) indicates that the introduction of adjusting factors changes the corrections by  $\alpha^r$  times, where  $r$  – the correction number.

$$\text{Thus, } \mathbf{X}^* = \mathbf{X}_0 + \sum_r \alpha^r \Delta\mathbf{X}_r.$$

Enumeration of  $\alpha$  can always provide convergence of the series, and when the intermediate point  $\mathbf{X}^*$  is found, one can start searching for a solution  $\mathbf{X}_p$  or the next intermediate point, if the series converges unsatisfactorily. As a result, we will either obtain a solution or the search process will 'hang' at some limit point  $\mathbf{X}_L$ , if there is no solution. The latter manifests itself in that the coefficients  $\alpha$ , ensuring the convergence of the intermediate series, start tending to zero, while the sequence of intermediate points tend to point  $\mathbf{X}_L$ , where the Jacobian of steady-state equation vanishes.

Reliable convergence of the series is ensured when  $\alpha$  is chosen by the condition

$$\alpha = \sqrt{\beta \frac{\|\Delta\mathbf{X}_1^{(k)}\|}{\|\Delta\mathbf{X}_p^{(k)}\|}}$$

where  $0 < \beta < 1$  – the coefficient ensuring a set speed of the series convergence;

$$\|\Delta \mathbf{X}_1^{(k)}\| = \left\{ \sum_{i=1}^n [\Delta \mathbf{X}_{1i}^{(k)}]^2 \right\}^{\frac{1}{2}} ; \|\Delta \mathbf{X}_p^{(k)}\| = \left\{ \sum_{i=1}^n [\Delta \mathbf{X}_{pi}^{(k)}]^2 \right\}^{\frac{1}{2}}$$

– norms of the vectors of the first and higher-order corrections.

The next approximation of the vector of dependable variables is calculated as follows:

$$\mathbf{X}^{(k)} = \mathbf{X}^{(k)} + \sum_{r=1}^p \frac{1}{r!} \alpha^r \Delta \mathbf{X}_r^{(k)}.$$

A large group of starting algorithms can be implemented using the steady-state equation solving methods based on the minimization of residual vector norm [22]. Computational experiments indicate that when the starting algorithms are used, high accuracy is not required, it is sufficient to obtain approximated values lying in a wide neighborhood of the desired solution.

The use of X parameters calculated using the starting algorithms as initial approximations when solving equations 14 or 18, ensures reliable convergence to the required points  $\mathbf{Y}_L^{(nb)}$ , lying on the 'near' boundaries of the stability region (Fig. 5).

In [7], the authors propose the equations which can be used to determine the limit conditions satisfying extreme values of functionals that depend on controlled and non-controlled operating parameters. These equations can be used to implement a technique of selecting optimal control actions of emergency control equipment that will provide the minimal damage caused by generator tripping and load shedding to perform the emergency control actions. It is also possible to take into account the damage due to variations in voltage at the nodal points of the network and frequency in the electric power system. A distinctive feature of the proposed technique of choosing optimal

control actions is the absence of multi-step optimization procedures and numerical differentiation. The search for the optimal solution is carried out by solving a system of equations with quadratic nonlinearity using Newton's method.

#### IV. DYNAMIC TRANSITION IN THE CASE OF REDUCTION IN GENERATOR POWER

A qualitative dynamic transition during the reduction in power of synchronous generators can be performed based on the optimal tuning of AVR and ASR [9, 12]. In this case, the coordinated tuning of AVR and ASR becomes particularly important, which is associated with the relatively low power of distributed generators and low inertia constant of their rotors. The principle of harmonized tuning implies the determination of optimal tuning factors for AVR and ASR which ensure minimal voltage and frequency deviations from the set values, as well as high damping properties during electrical transient processes, which is confirmed by the studies performed on simulation models of EPS with DG plants [9, 12, 13, 18].

The AVR and ASR settings are harmonized in two steps [9]: identification of 'turbine-generator' model based on the experimental data using wavelet transform; search for optimal setting of regulators using genetic algorithm [9–12] and determination of the oscillatory stability margin.

For identification, a model of the closed-loop system of the DG plant control is built using the experimental data. To this end, apriori information is used to determine numeric values of complex transfer factors of the DG plant transfer function matrix, as a relation of spectrums of relevant output and input signals of the closed-loop 'turbine-generator' system (Fig.6).

The characteristic polynomial of the considered system is determined using the following expression:

$$D^M(j\omega) = \det[\mathbf{E} + \mathbf{W}_G(j\omega) \cdot \mathbf{W}_R(j\omega)] \quad (21)$$

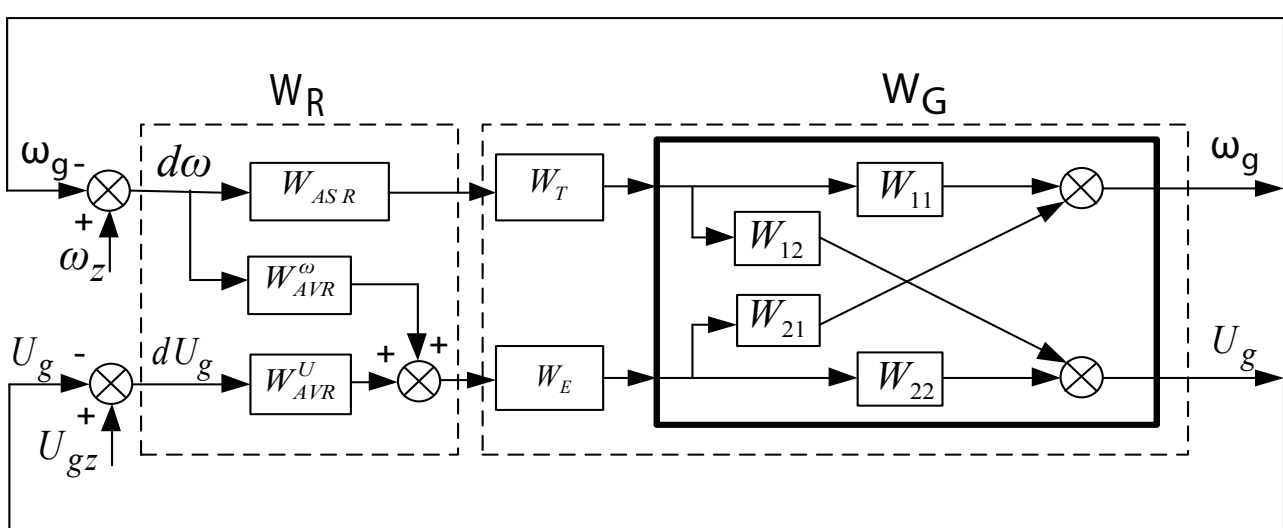


Fig. 6. The 'turbine-generator' system structural diagram:  $W_T$  – complex turbine gear ratio;  $W_E$  – complex exciter gear ratio.

where  $\mathbf{W}_G(j\omega)$  – matrix transfer function of the controlled object ('turbine-generator' system), which is determined experimentally;  $\mathbf{W}_R(j\omega)$  – regulator matrix transfer function that takes into account relationship between AVR and ASR, and includes the required tuning coefficients:

$$\mathbf{W}_R(j\omega) = \begin{bmatrix} W_{ASR}(j\omega) & W_{AVR}^\omega(j\omega) \\ 0 & W_{AVR}^U(j\omega) \end{bmatrix}; \quad W_{ASR}(j\omega) - \text{ASR}$$

complex transfer factor;  $W_{AVR}^\omega(j\omega)$  – complex transfer factor for frequency-tuned AVR channel;  $W_{AVR}^U(j\omega)$  – complex transfer factor for AVR voltage-tuned channel.

Experimental determination of DG plant matrix transfer function allows taking into account the influence of other DG plants and relation with EPS in possible steady-state conditions of the power supply system.

An approach is proposed to obtain accurate complex transfer factors of the DG plant. In this approach, the testing effect occurs on the basis of the regulator noise [9] detected using the wavelet transform. The technique of regulator noise detection with wavelet transform includes the following steps:

1. Select a basic wavelet and decomposition level  $N$ ; perform wavelet decomposition of signal  $f(t)$  to level  $N$ ;
2. Set a threshold for each level and process the detail coefficients;
3. Reconstruct wavelet by using initial approximating factors of level  $N$  and modified detail coefficients of levels  $1 \dots N$ ;

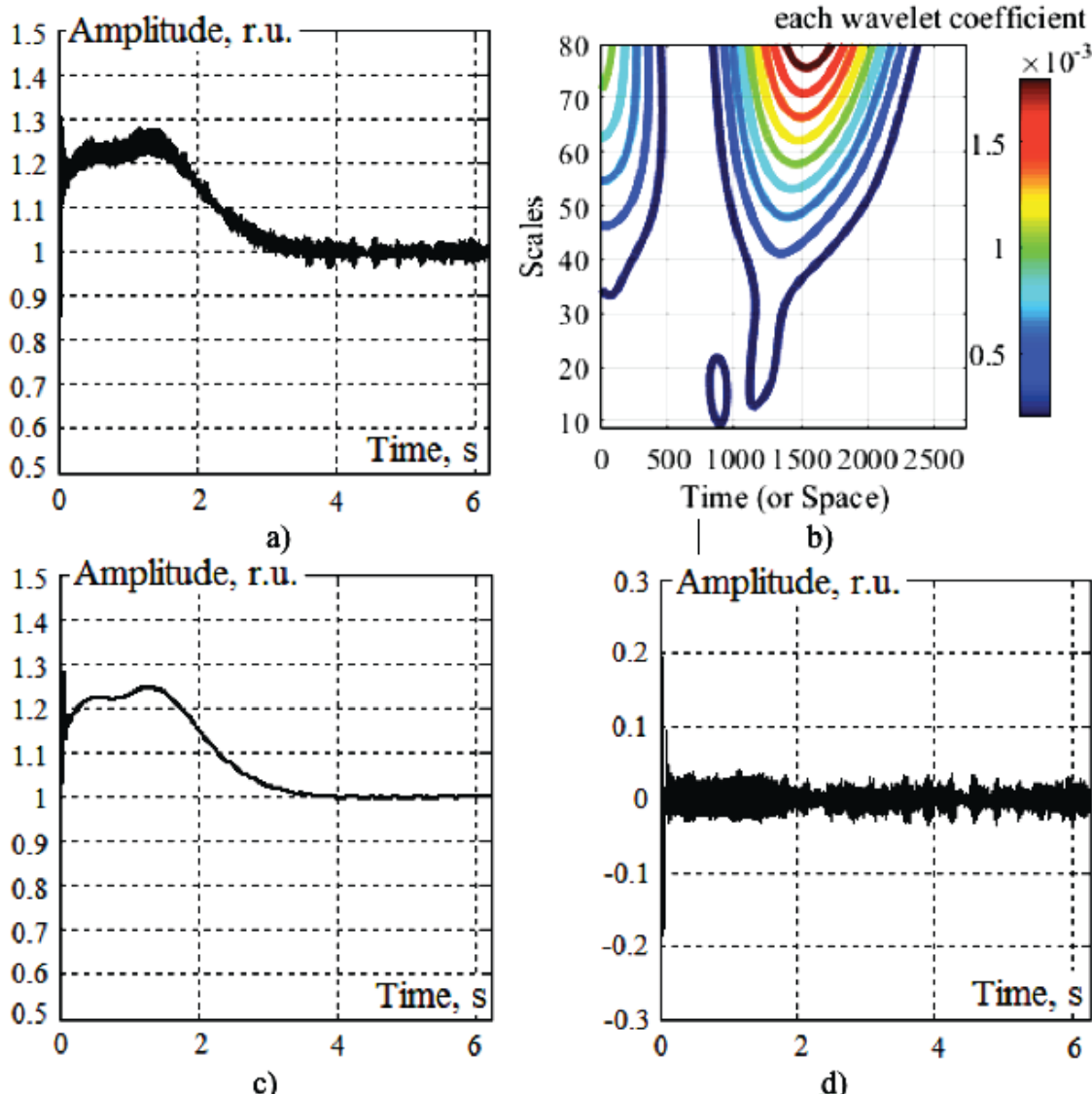


Fig. 7. Regulator noise detection using wavelet transform technology: a) initial regulator signal with noise; b) scaling-gram of the initial regulator signal with noise; c) the detected useful signal; d) regulator noise.

4. Detect signal noise used for identification:

$f_v(t) = f(t) - f_w(t)$ , where  $f_w(t)$  – useful signal component obtained with the wavelet transform;  $f_v(t)$  – noise.

Figure 7 shows the effectiveness of wavelet transform technology for detection of regulator noise when used for identification: initial regulator signal containing noise; scalinggram of the initial noisy regulator signal, whose uneven lines are indicative of the noise presence; the detected useful signal and regulator noise. Daubechies [23] wavelet was used as a basic one.

The AVR and ASR settings of DG plant generator are optimized using the genetic algorithm (GA) with the following quadratic criterion [9]:

$$J = \int_0^{\Omega} e^2(j\omega) d\omega \rightarrow \min \quad (22)$$

where  $e(j\omega) = D^D(j\omega) - D^M(j\omega)$  – mismatch between the desired set of values  $D^D(j\omega)$  and model set  $D^M(j\omega)$  of characteristic polynomials;  $\omega$  – actual frequency value from a range  $[0; \Omega]$  determined by the system 'bandwidth'. Newton's or Butterworth polynomials can be used as desired polynomials.

Optimization criterion (22) has a large number of local extrema, consequently, it is advisable to use the genetic algorithm to search for a global minimum in the presented task. This algorithm represents an optimum search technique based on the mechanisms of natural selection and inheritance. The main idea of GA was first proposed by J. Holland in 1975 [24]. This idea was further developed in the works by his followers: Goldberg and de Jong [25, 26].

Because the mismatch value  $e(j\omega) = \text{Re}(\omega) + j\text{Im}(\omega)$  is a complex one, it is difficult to minimize functional (22). Therefore, it is advisable to use linear convolution:

$$J = \frac{1}{2} J_{\text{Re}} + \frac{1}{2} J_{\text{Im}} \rightarrow \min \quad (23)$$

where  $J_{\text{Re}}$ ,  $J_{\text{Im}}$  – criteria satisfying the proximity of hodographs in the regions of real and imaginary values. These criteria are formed as follows:

$$J_{\text{Re}} = \int_0^{\Omega} (\text{Re}D^D(\omega) - \text{Re}D^M(\omega))^2 d\omega \quad (24)$$

$$J_{\text{Im}} = \int_0^{\Omega} (\text{Im}D^D(\omega) - \text{Im}D^M(\omega))^2 d\omega \quad (25)$$

Characteristic hodograph of system (21) with determined AVR and ASR tuning coefficients allows judging on stability and other dynamic properties in a limited frequency range. In particular, the stability of distributed generators can be estimated with respect to the rate of change in the phase of characteristic hodograph (21) using the curve analysis method [27] proposed by Bushuev V.V.:

$$V(\omega) = \left[ \frac{d\varphi_D(\omega)}{d\omega} \right]^{-1} \quad (26)$$

where  $\varphi_D(\omega)$  – phase-frequency characteristic determined by the system frequency hodograph.

When frequency  $\omega_p$  reflects the equivalent frequency of system self-oscillations, characteristic (26) determines the real part of some equivalent root, which can be used to assess the extent to which the system is stable.

The method of harmonized AVR and ASR tuning allows determining the optimal tuning coefficients of regulators for different operating conditions of the power system and forming a basis of rules for the fuzzy control system. To this end, the use of an auto-tuning unit with the modules of operating condition identification and harmonized tuning of regulators is proposed. Figure 8 shows a block diagram of the proposed fuzzy control system.

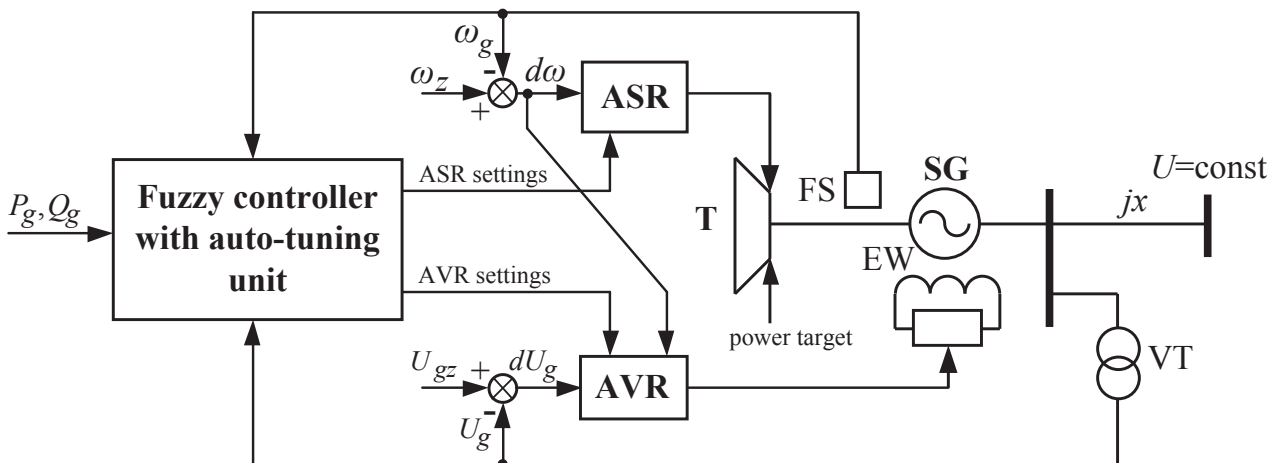


Fig. 8. Structural scheme of the fuzzy control system of AVR and ASR of the DG plant: FS - frequency sensor; EW - excitation winding; SG - synchronous generator; T - turbine; VT - voltage transformer.

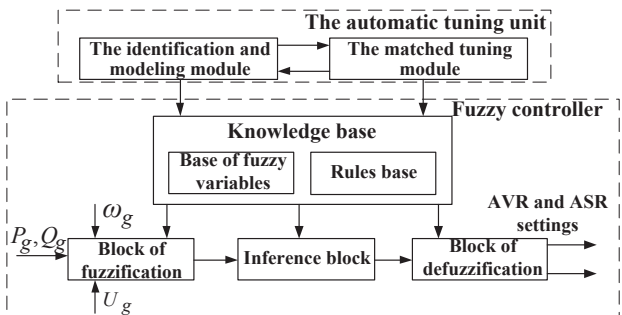


Fig. 9. The block diagram of the fuzzy control system with self-tuning unit.

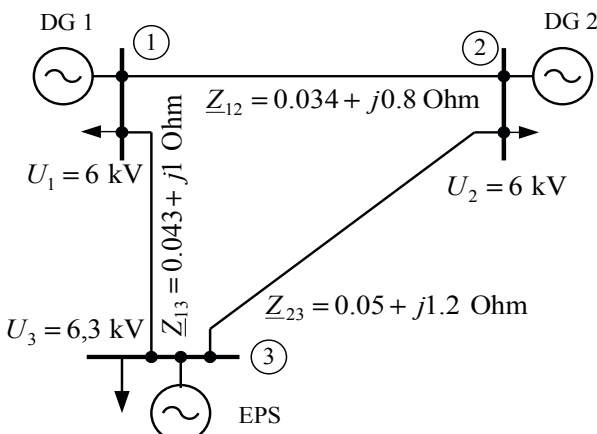


Fig. 10. Diagram of the considered power system.

The input parameters of the fuzzy control system are the actual values of voltage  $U_g$ , rotor speed  $\omega_g$ , and powers  $P_g, Q_g$  of DG plant. The fuzzy control system determines AVR and ASR tuning coefficients that are optimal for a current

condition. This system with a self-tuning unit is a system of fuzzy logic inference with modules of identification and harmonized tuning of AVR and ASR (Fig.9) [12, 13]. The self-tuning unit consists of an identification and modeling module and a module of harmonized tuning which allow it to form a knowledge base for the fuzzy control system of AVR and ASR settings in different operating conditions of the DG plant.

#### V. THE MODELING RESULTS

Modeling was carried out for the power system shown in Fig. 10. In the power system in question, there are two mini hydropower plants with a capacity of 24 MW each, operating for the industrial lumped load (timber processing facilities) connected at nodes 1 and 2. The facilities operate in one shift, and in the evening peak hours in the EPS, each generator supplies 15 MW to the receiving system (node 3). The network is implemented via flexible symmetrical electrical pathways [28]. Tripping of line 1-3 was considered as an emergency condition.

The post-emergency conditions meeting the stability constraints using the set and shortest paths that are calculated with equations (14) and (18) are shown in Fig.11. The initial loading condition of the DG plant generators is represented by a point with coordinates  $\mathbf{Y}^0 = [20 \ 20]^T$ ; the calculation of the operating conditions meeting the stability constraints using the set path is represented by point  $\mathbf{Y}_{L1} = [12,9 \ 20]^T$ , and with the shortest path –  $\mathbf{Y}_{L2} = [16,56 \ 16,45]^T$ ; additional reduction in generator power that ensures the necessary stability margin corresponds to the points  $\mathbf{Y}_{Z1} = [10,8 \ 17,85]^T$ ;  $\mathbf{Y}_{Z2} = [10,8 \ 17,85]^T$  (Fig. 11).

The multiple computer-aided experiments indicate that

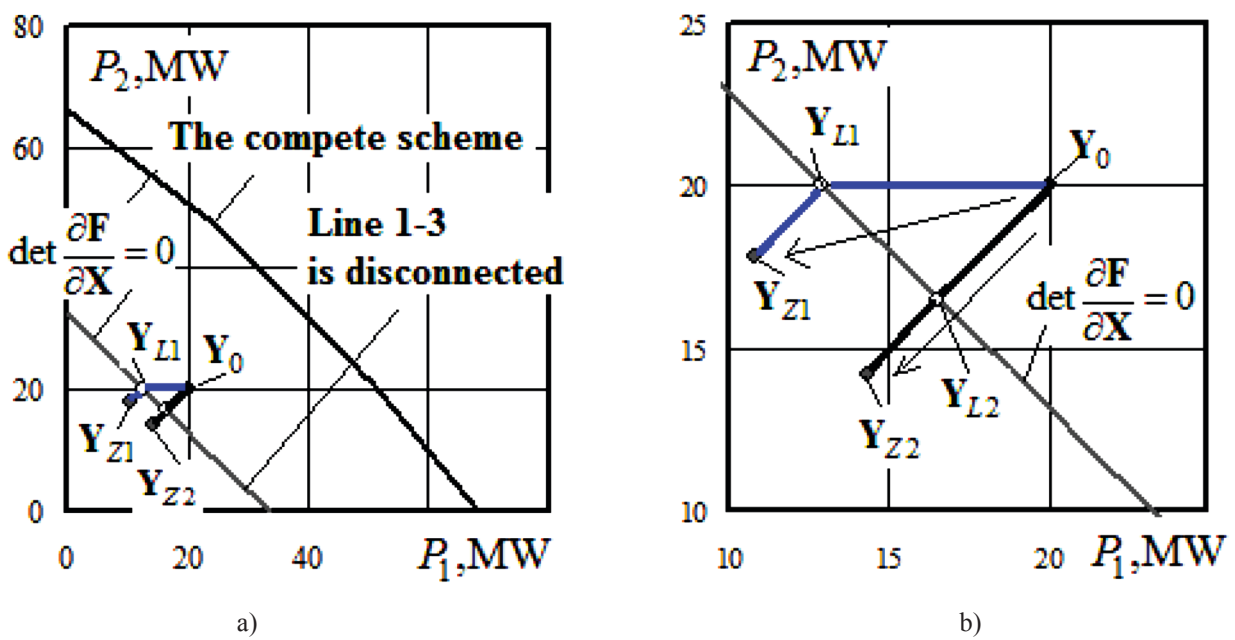


Fig. 11 Calculation of operating conditions meeting the stability constraints, using limit load equations.

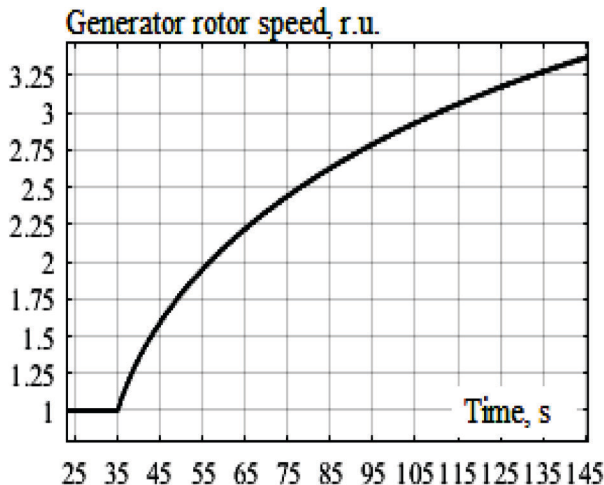


Fig. 12 Oscillogram of generator rotor speed of the DG plant 1, without AVR and ASR when line 1-3 is disconnected

the use of the limit load equations and starting algorithm based on minimization of functional residuals makes it possible to calculate the required boundary value of the stability region.

Additionally, the MATLAB-based modeling was carried out given the models of AVR and ASR defined with the following complex transfer factors:

$$W_{\text{ASR}}(j\omega) = \left( k_p + \frac{k_i}{0.1j\omega} + \frac{k_d j\omega}{j\omega+1} \right) \cdot \frac{1}{0.01j\omega+1}$$

$$W_{\text{AVR}}^{\omega}(j\omega) = \frac{1+0.5j\omega}{0.5j\omega} \left[ \frac{2k_{0\omega}j\omega}{(2j\omega+1)(0.02j\omega+1)} + \frac{0.05k_{1\omega}j\omega}{0.05j\omega+1} \right]$$

$$W_{\text{AVR}}^U(j\omega) = \frac{1+0.5j\omega}{0.5j\omega} \cdot \left( k_{0u} - \frac{0.02k_{1u}j\omega}{0.06j\omega+1} \right)$$

where  $k_p$ ,  $k_i$ ,  $k_d$  – ASR tuning coefficients;  $k_{0\omega}$ ,  $k_{1\omega}$ ,  $k_{0u}$ , and  $k_{1u}$  – tuning coefficients for AVR adjusting channels.

A detailed description of the used model of regulators is given in [9, 12, 13]. The method of harmonized tuning was

used to determine the parameters of the regulators for three loads of the generators (minimum load, average load, and maximum load). These parameters were then used to build a rule base for the fuzzy control system.

The modeling results show that without AVR and ASR, disconnection of one line causes instability of generators. The corresponding oscillogram of generator rotor speed for DG plant 1 is shown in Fig. 12. This is due to the relatively low power of the generators and the low constant inertia of their rotors, which require fast and coordinated control.

Modeling involved the calculation of the DG plants operating conditions meeting the stability constraints for the case of a short circuit on line 1-3, which occurs in electric power system, and its disconnection by relay protection in 0.3 s. When DG plants operate without regulators, disconnection of one line causes stability loss in the system. To ensure stability in the post-emergency conditions, it is necessary to reduce the power of the DG plant generators. In this case, the correctness of DG plants AVR and ASR settings influences greatly the quality of the system dynamic transition. As an example, oscillograms of generator speed and active power of DG plant 1 are given. They indicate a negative effect of non-harmonized settings of regulators on the quality of the transient process (Fig. 13).

Harmonized settings of AVR and ASR and their change in different operating conditions of generators considerably improve the quality indices of transient processes. The corresponding oscillograms of voltage, frequency, and power of the DG plants for the case of short circuit and tripping of line 1-3 are shown in Figs. 14 and 15. The main advantage of the change in the AVR and ASR settings in different operating conditions is a decrease in oscillation, overshoot and time of the transient process for voltage, frequency, and power of the DG plant, which ensures a qualitative dynamic transition when generator power is reduced in the post-emergency conditions.

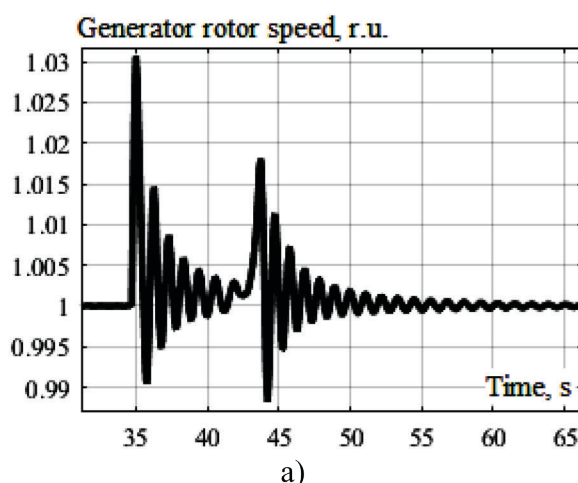


Fig. 13. Oscillograms of generator rotor speed (a) and active power (b) of DG plant 1 for non-harmonized AVR and ASR settings (the operating conditions meeting stability constraints are calculated using the shortest path).

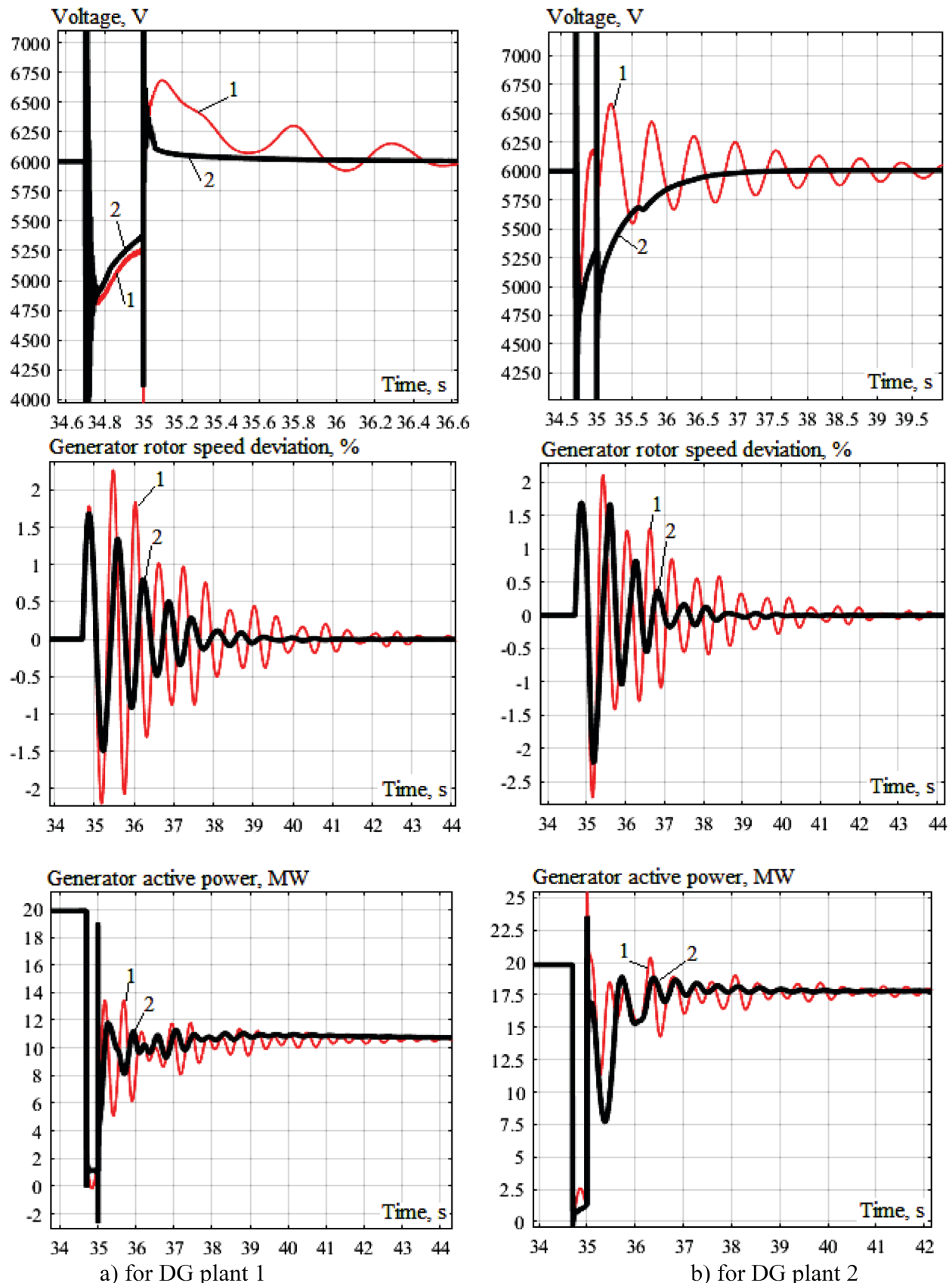


Fig. 14. Oscillograms for voltage, frequency, and power of DG plants in the case of tripping line 1-3 (the operating conditions meeting the stability constraints are calculated using the set path): 1 – without changes in the AVR and ASR tuning coefficients; 2 – using a fuzzy controller that changes the AVR and ASR settings.

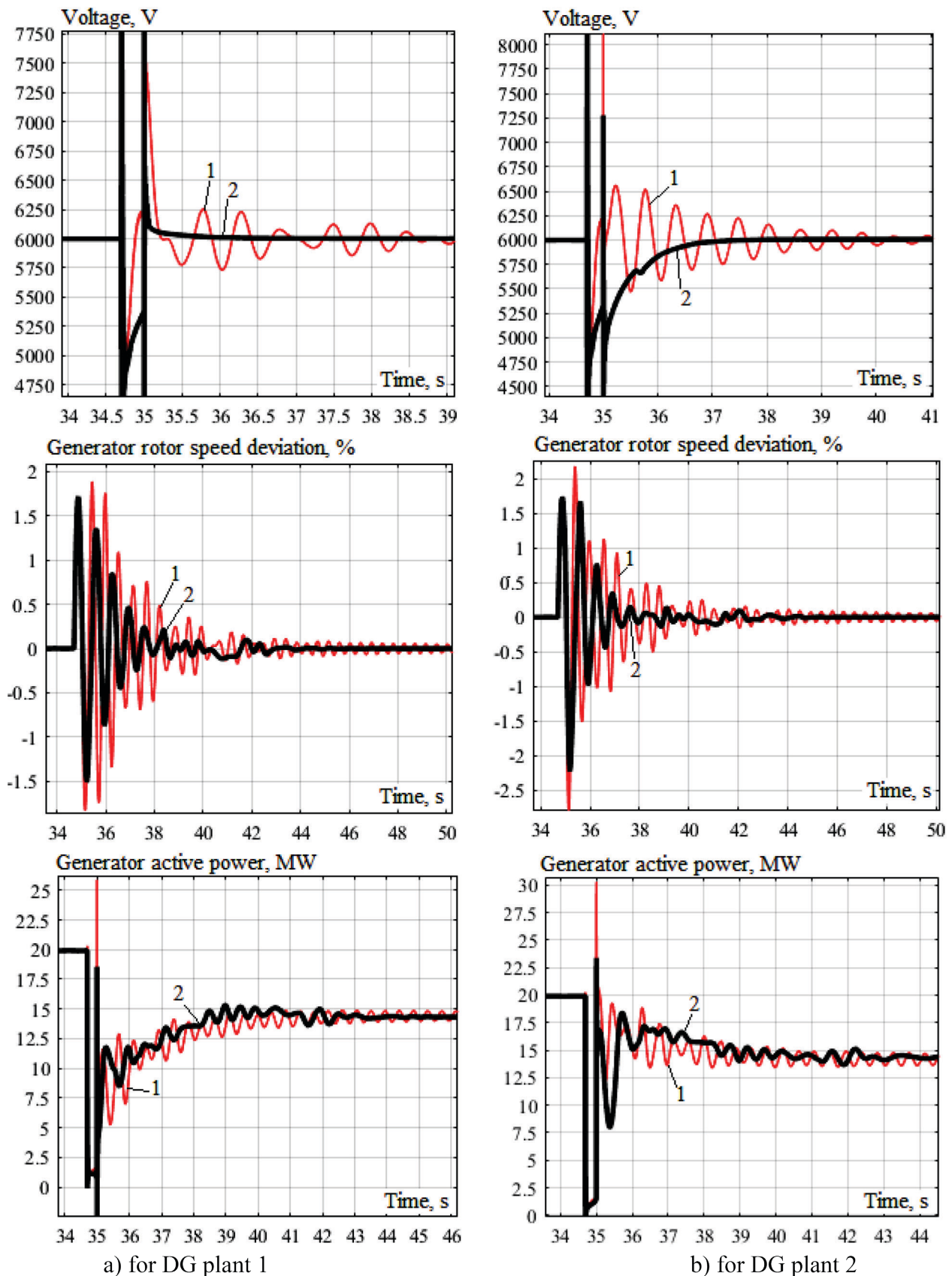


Fig. 15. Oscillograms for voltage, generator rotor speed deviation and power of DG plants in the case of tripping line 1-3 (the operating conditions meeting the stability constraints are calculated by the shortest path): 1 – without changes in the AVR and ASR tuning coefficients; 2 – using a fuzzy controller that changes the AVR and ASR settings.

## VI. CONCLUSION

The paper presents the methods for calculating the operating conditions meeting the stability constraints based on the limit load equations that can be used in the emergency control to be performed by distributed generation plants. A fuzzy control system is proposed to control the parameters of the DG plant regulators. The knowledge base of this system allows the formation of a self-tuning unit based on the application of AVR and ASR harmonized tuning technique using wavelet transform and genetic algorithm.

Based on the performed calculations and computer modeling, the following conclusions can be drawn:

1. The post-emergency conditions meeting the stability constraints can be effectively calculated using the limit load equations with the aid of a starting algorithm that enables the operating condition to reach the near boundary of the stability region.
2. Harmonized tuning of generator regulators provides a good quality of dynamic transition along the set path when DG plants generator power is reduced in post-emergency operating conditions.
3. Application of fuzzy algorithms to control AVR and ASR settings considerably enhances the quality of voltage, frequency and power transient processes when the power of DG plant generators is reduced in the post-emergency conditions.

## REFERENCES

- [1] Innovative Power Engineering - 21 / Ed. V.M. Batenin, V.V. Bushuev, N.I. Voropai, Information Center *Energia*, Moscow, 2017, 584 p. (in Russian)
- [2] N.I. Voropai, Z.A. Stychinsky, Renewable energy sources: theoretical foundations, technologies, technical characteristics, economics, *Otto-von-Guericke-Universität*, Magdeburg, 2010, 223 p.
- [3] N.I. Voropai, V.G. Kurbatsky, N.V. Tomin [and others], Complex of intelligent tools for the prevention of major accidents in power systems, *Nauka*, Novosibirsk, 2016, 332 p. (in Russian)
- [4] K. Suslov, N. Solonina, V. Stepanov, "A principle of power quality control in the intelligent distribution networks", in Proc. *International Symposium on smart electric distribution systems and technologies*. (EDST 2015), 2015, pp. 260-264.
- [5] I.Z. Gluskin, B.I. Iofyev, Emergency automation in power systems, *Znak*, Moskow, T.1, 2009, 568 p. (in Russian)
- [6] I.Z. Gluskin, B.I. Iofyev, Emergency automation in power systems, *Znak*, Moskow, T.2, 2011, 528 p. (in Russian)
- [7] A.V. Kryukov, Limiting regimes of electric power systems, Irkutsk: *IrGUPS*, 2012, 236 p. (in Russian)
- [8] A.N. Belyaev, S.V. Smolovik, "Designing adaptive automatic excitation controllers using neuro-fuzzy modeling", *Electricity*, No. 3, pp. 2-9, 2002. (in Russian)
- [9] Yu.N. Bulatov, A.V. Kryukov, "Application of wavelet transform and genetic algorithms to tune automatic regulators of distributed generation plants", *Scientific Bulletin of NSTU*, Vol.63, No. 2, pp. 7-22, 2016. (in Russian)
- [10] Chen Y., Ma Y., Yun W. "Application of Improved Genetic Algorithm in PID Controller Parameters Optimization", *Telkomnika*, Vol. 11, No. 3, pp. 1524-1530, 2013.
- [11] Jaen-Cuellar A.Y., Romero-Troncoso R. de J., Morales-Velazquez L., Osornio-Rios R.A. "PID-Controller Tuning Optimization with Genetic Algorithms in Servo Systems", *International Journal of Advanced Robotic Systems*. Vol. 10, pp. 324-337, 2013.
- [12] A.V. Kryukov, S.K. Kargapol'tsev, Yu.N. Bulatov, O.N. Skrypnik, B.F. Kuznetsov, "Intelligent control of the regulators' adjustment of the distributed generation installation", *Far East Journal of Electronics and Communications*, Vol.17, No. 5, pp. 1127-1140, 2017.
- [13] Yury N. Bulatov, Andrey V. Kryukov, "Neuro-Fuzzy Control System for Distributed Generation Plants", Proceedings of the Vth International workshop "Critical infrastructures: Contingency management, Intelligent, Agent-based, Cloud computing and Cybersecurity" (IWCI 2018), *Atlantis Press, Advances in Intelligent Systems Research*, Vol. 158, pp. 13-19, 2018.
- [14] Yu.N. Bulatov, A.V. Kryukov, K.V. Suslov, "Multi-agent technologies for control of distributed generation plants in the isolated power systems", *Far East Journal of Electronics and Communications*, Vol. 17, No. 5, pp. 1197-1212, 2017.
- [15] E.F. Camacho, C. Bordons, *Model Predictive Control*. 2nd edition Springer, 2007, 405 p.
- [16] J. Wang, A.Q. Huang, W. Sung, Y. Liu, B.J. Baliga, "Smart Grid Technologies", *IEEE Industrial Electronics Magazine*, Vol. 3, No.2, pp. 16-23, 2009.
- [17] Ran Wang, Ping Wang, Gaoxi Xiao, Intelligent Microgrid Management and EV Control Under Uncertainties in Smart Grid, *Springer*, 2018, 218 p.
- [18] Yuri N. Bulatov, Andrey V. Kryukov, Konstantin V. Suslov, "Solving the flicker noise origin problem by optimally controlled units of distributed generation", *Proceedings of International Conference on Harmonics and Quality of Power (ICHQP) 2018*, pp. 1-4, 2018.
- [19] A.M. Kontorovich, A.V. Kryukov, "The use of equations of limiting regimes in problems of control

- of power systems”, Izv. Academy of Sciences of the USSR, *Energy and transport*, No.3, pp. 25-33, 1987. (in Russian)
- [20] A.M. Kontorovich, A.V. Kryukov, Yu.V. Makarov, et al., Methods for calculating on the computer of the sustainability of complex energy systems, Irkutsk: *Irkutsk University Press*, , p. 89, 1988.
- [21] B.I. Ayuyev, V.V. Davydov, P.M. Erokhin, “Optimization model of limiting modes of electrical systems”, *Electricity*, No.11, pp.3-11, 2010. (in Russian)
- [22] V.I. Tarasov, Theoretical bases of the analysis of the steady-state regimes of electric power systems, *Nauka, Novosibirsk*, 2002, 344 p. (in Russian)
- [23] I. Dobeshi, Ten lectures on wavelets, *RHD*, Moskow, 2001, 464 p. (in Russian)
- [24] J.H. Holland, Adaptation in Natural and Artificial Systems, Cambridge, MA: *MIT Press*, 1975, 183 p.
- [25] D.E. Goldberg, “Simple genetic algorithms and the minimal deceptive problem”, Genetic Algorithms and Simulated Annealing. Chapter 6, *Los Altos, CA, Morgan Kauffman*, pp. 74-88, 1987.
- [26] D.E. Goldberg, Genetic algorithm in search, optimization and machine learning, MA: *Addison-Wesley Longman Publishing Co.*, 1989, 322 p.
- [27] V.V. Bushuev, Dynamic properties of electric power systems, *Energoatomizdat*, Moskow, 1987, 120 p. (in Russian)
- [28] A.M. Semchinov, Conduits of industrial enterprises, Energy, 1972, 200 p. (in Russian)



**Yury Bulatov** is Head of the Department of Power Industry and Electrical Engineering at Bratsk State University, Russia. He graduated from Bratsk State University in 2007. Yury Bulatov received his degree Candidate of Technical Sciences from Irkutsk State Transport University in 2012. His research interests include modeling of power and control systems, modeling and control of electric power system operating conditions; power grids; smart grids.



**Andrey Kryukov** is Professor of the Transport Electric Engineering Department at Irkutsk State Transport University, Professor of the Power Supply and Electrical Equipment Department at Irkutsk National Research Technical University, Russia. He graduated from East Siberian Technological Institute in 1974. Andrey Kryukov received his degrees of Candidate of Technical Sciences from Leningrad Polytechnic Institute in 1982 and Doctor of Technical Sciences from Energy Systems Institute SB RAS in 1997. His research interests are modeling and control of electric power systems and power supply systems of the railroads; smart grids.